

Computational Investigations of the Bonding Layer in CVD-Coated WC+Co Cutting Tools

Zhi-Jie Liu, Charles McNerny, Pankaj Mehrotra, Yi-Xiong Liu, and Zi-Kui Liu

(Submitted October 21, 2005; in revised form November 11, 2005)

The effect of processing parameters on the bonding layer structure of the chemical vapor deposition (CVD) coated cemented carbide inserts was investigated through thermodynamics calculations. It was found that, under equilibrium conditions, the existing processing parameters would deposit graphite. To eliminate the thermodynamic driving force for the formation of graphite, the amount of the methane participating in equilibrium calculations must be significantly reduced. Under such circumstances, various titanium carbides formed instead, in agreement with recent experimental investigations. Thus the methane may have not fully cracked during the CVD coating process.

Keywords Al₂O₃, bonding layer, chemical vapor deposition

1. Introduction

Today, about 60% of cemented carbide cutting tools are chemical vapor deposition (CVD) coated^[1] with a top Al₂O₃ layer for excellent wear-resistance. There are typically two forms of Al₂O₃ phases: the stable α - and metastable κ -Al₂O₃ phases. Although the α -Al₂O₃ phase shows excellent high temperature stability, it is difficult to form and has relatively poor adhesion to the inner nonoxide layer compared with the κ -Al₂O₃ phase. Therefore, a so-called bonding layer was used before the deposition of the Al₂O₃ layer to favor the formation of the α -Al₂O₃ phase and improve its adhesion to the inner nonoxide layer.^[2,3] In our previous experimental investigation,^[4] it was found that, under typical CVD processing conditions for the bonding layer, various titanium oxides were observed instead of the commonly believed Ti(C,N,O) phase.^[5,6] To fully understand phase stability in bonding layers in CVD coating of cemented carbide cutting tools, detailed thermodynamic calculations are carried out in the present work to investigate the effects of various processing parameters.

2. Calculation Procedures

In our previous experimental investigation, a laboratory-scale CVD cylinder was used. Feeding gases flowed upward in the chamber at 60 torr pressure with a temperature of

This paper was presented at the International Symposium on User Aspects of Phase Diagrams, Materials Solutions Conference and Exposition, Columbus, Ohio, 18-20 October, 2004.

Zhi-Jie Liu and Zi-Kui Liu, Department of Materials Science and Engineering, The Pennsylvania State University, University Park, PA 16802; and Charles McNerny, Pankaj Mehrotra, and Yi-Xiong Liu, Kennametal, Inc., Corporate Technology, Latrobe, PA 15650. Contact e-mail: zikui@psu.edu.

970 °C at the bottom and 1000 °C at the top of the chamber.^[4] The input gas mixture consisted of H₂ (86% volume), CH₄ (4%), CO₂ (1.7%), N₂ (8%), and TiCl₄ (0.3%). These experimental conditions were used as initial conditions in the present thermodynamic calculations using ThermoCalc software^[7] and the SGTE substance database^[8] combined with the FEDAT.^[9] As a first approximation, the Gibbs energy, $G_{\text{TiO}}^{\text{fcc}} = -430,000 + G_{\text{Ti}}^{\text{SER}} + 0.5 G_{\text{O}_2}^{\text{SER}}$ (J/mol of TiO) with the last two terms being the Gibbs energy of hcp-Ti and O₂, for the end-member of TiO in the Ti-O fcc phase and the interaction parameter, 8000 J/mol of formula in terms of the sublattice model (Ti)(O, Va), between oxygen and vacancy were estimated from those of the hcp phase in the Ti-O binary system.^[10] The effects of individual processing parameters, i.e., gas flow ratios defined by the initial concentrations in the input gas, temperature, and pressure, and their combinations on the phase stability were investigated by systematically varying their values.

3. Results and Discussion

In the previous experimental investigation,^[4] the bonding layers were deposited thicker than those on typical commercial cutting tools under the same conditions so they could be investigated by conventional x-ray diffraction (XRD). Four types of titanium oxides, i.e., TiO₂, Ti₄O₇, Ti₃O₅, and Ti₂O₃, were observed from the XRD analysis, while the equilibrium calculation showed three-phase equilibrium of gas, fcc, and graphite with the composition of fcc being Ti(C_{0.016}N_{0.984}) with almost no oxygen and the CH₄ concentration in the gas phase being 0.07%. It shows that over 98% of methane has been consumed. The calculated results are in contradiction to the experimental observations, particularly on the existence of graphite, which was not detected experimentally. Variations in temperature and pressure close to experimental values do not change the features of the three-phase equilibrium, as shown in Fig. 1 and 2 for pressure and temperature, respectively.

Consequently, the thermodynamic driving force for the formation of graphite with respect to gas flow ratios was

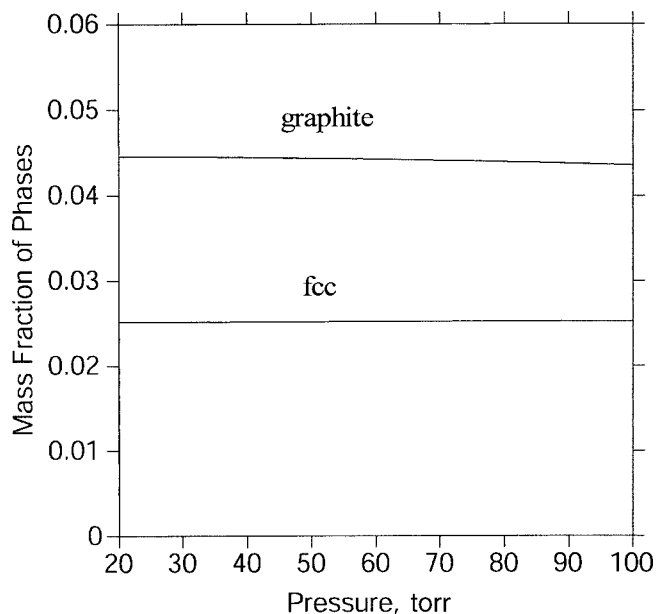


Fig. 1 Effect of pressure on mass fraction of phases at 970 °C

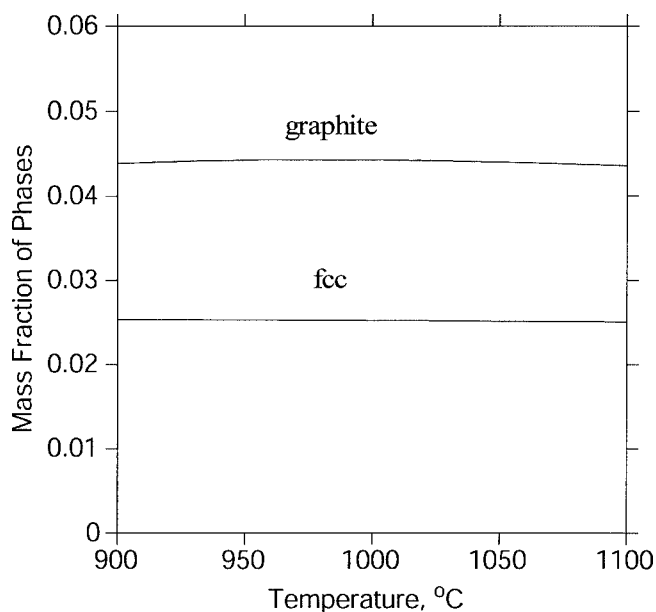


Fig. 2 Effect of temperature on mass fraction of phases at 60 torr

investigated. The expression for the driving force of graphite formation, D_{gra} , is represented by the following dimensionless quantity:

$$D_{\text{gra}} = -\frac{\Delta G}{RT} \quad (\text{Eq 1})$$

where ΔG stands for the Gibbs free energy change in the system when one mole of graphite is formed, and R and T are the gas constant and temperature. The driving force is

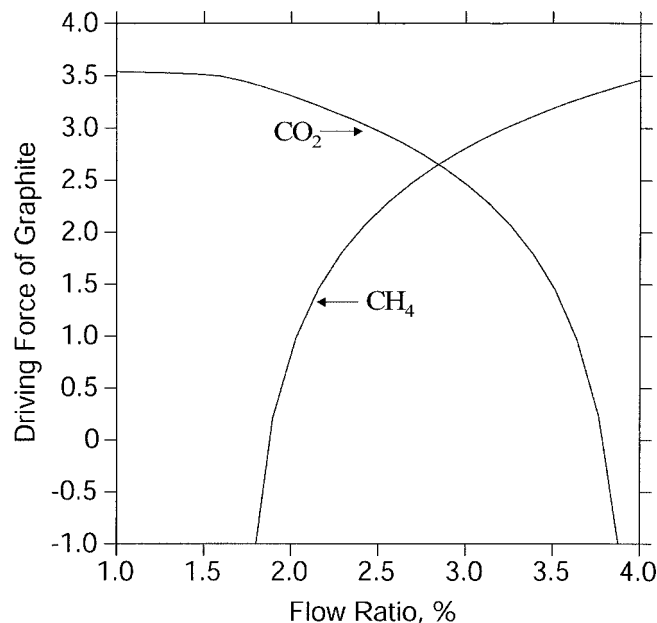


Fig. 3 Effect of gas flow ratios on the driving force of graphite at 970 °C and 60 torr

calculated by minimizing the system Gibbs energy without graphite participating in the equilibrium calculation. The difference between the Gibbs energy of graphite and the chemical potential of carbon in this equilibrium system is the ΔG in Eq 1. If D_{gra} is negative, then graphite will not form from the gas phase. It was found that only the flow ratios of CH_4 and CO_2 change the sign of D_{gra} , as indicated in Fig. 3. It should be mentioned that the change of flow ratios are realized by adjusting the flow rates of the respective gases with the input flow rates of other gases kept constant. This means that the flow ratios of all gases are changed simultaneously if the flow rate of one input gas is changed. It can be seen in Fig. 3 that, if the flow ratio of CH_4 is higher than 1.8%, the driving force for the formation of graphite will be positive, which means that the graphite will form from the gas phase. On the other hand, graphite will not form if the CH_4 flow ratio is lower than 1.8%. For CO_2 , the zero driving force point is around 3.7% with the higher CO_2 flow ratio preventing the formation of graphite due to the formation of more CO along with a dramatic decrease of the CH_4 partial pressure in the gas phase. Such calculations may indicate that the dominant sooting reaction may be the decomposition of CH_4 and addition of more CO_2 has the effect of consuming more CH_4 because CH_4 reacts with CO_2 to form carbon monoxide. It should be mentioned that these calculations represent chemical potential differences of carbon between graphite and the equilibrated fcc-gas two-phase mixture under various conditions without knowing the details of reaction paths; however, these calculations can provide information on possible reaction paths.

In experiments, the flow ratios of CH_4 and CO_2 are 4% and 1.7%, respectively. Because a flow ratio of CO_2 higher than the experimental value is needed to reduce the stability of graphite, the flow ratio of CO_2 cannot contribute to the

Section I: Basic and Applied Research

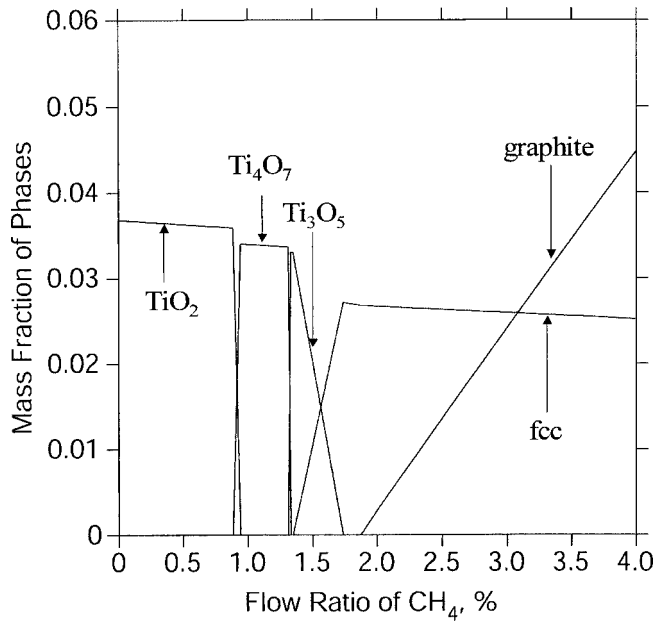


Fig. 4 Phase fractions as a function of CH_4 flow ratio at 970°C and 60 torr

lack of graphite in experimental observations. For CH_4 , the flow ratio of 1.8% for the zero driving force is lower than the experimental value of 4%. Therefore, if less than 45% of all CH_4 molecules are active in chemical reactions in the system, the driving force for the formation of graphite can become negative. The phase fractions as a function of the CH_4 flow ratio are plotted in Fig. 4. In addition to the disappearance of graphite, it is observed that the fcc phase is not stable when the flow ratio of CH_4 is lower than 1.36%, and various titanium oxides become stable at lower flow ratios of CH_4 .

To study the combined effect of temperature and CH_4 , the phase diagram of the CH_4 flow ratio and temperature was calculated and plotted (Fig. 5). In the temperature range from 970 to 1000°C and the flow ratio of CH_4 from 0 to 1.36% are five phase regions: gas+ TiO_2 , gas+ $\text{TiO}_2+\text{Ti}_4\text{O}_7$, gas+ Ti_4O_7 , gas+ $\text{Ti}_4\text{O}_7+\text{Ti}_3\text{O}_5$, and gas+ Ti_3O_5 . If the flow ratio of CH_4 locates in the gas+ $\text{TiO}_2+\text{Ti}_4\text{O}_7$ phase region, both TiO_2 and Ti_4O_7 oxides will co-deposit from the gas phase to form the bonding layer. On the other hand, if there is a local variation of the flow ratio of CH_4 between the gas+ TiO_2 and gas+ Ti_4O_7 phase regions, a mixture of TiO_2 and Ti_4O_7 could also be achieved. Similarly, if there is a local variation of the flow ratio of CH_4 in the gas+ TiO_2 and gas+ Ti_3O_5 phase regions, a mixture of TiO_2 and Ti_3O_5 oxides could be found in the bonding layer.

To investigate the decomposition of CH_4 , Fulcheri and Schwob^[11] considered the following chemical reaction: $\text{CH}_4 \rightarrow \text{C} + 2\text{H}_2$. This reaction is endothermic, and the standard decomposition enthalpy, ΔH° , is 74.6 kJ/mol. Fulcheri and Schwob plotted the energy supply needed for the above reaction as a function of temperature and concluded that the temperature should be between 1000 and 2000°C for the reaction to take place. Moradov mentioned that the processing temperatures for this decomposition re-

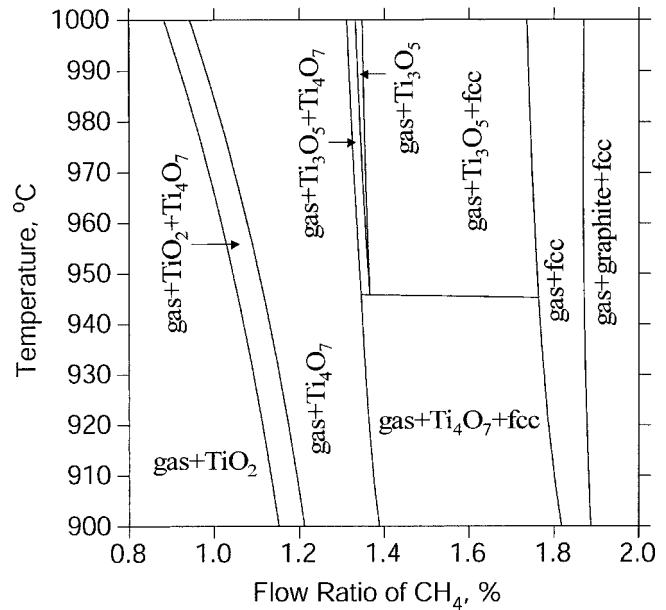


Fig. 5 Effect of temperature and CH_4 flow ratio on formation of titanium oxides at 970°C and 60 torr

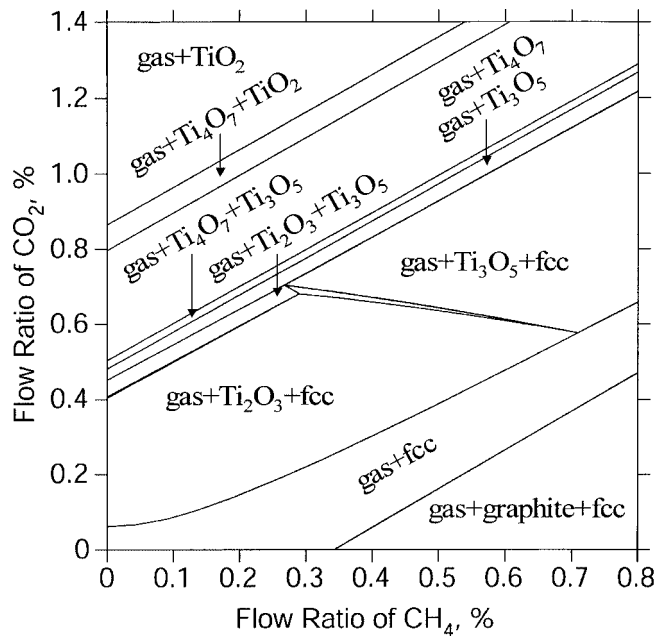


Fig. 6 Effect of CO_2 and CH_4 flow ratios on the formation of titanium oxides with TiCl_4 gas flow ratio = 0.3%, $T = 970^\circ\text{C}$, and $p = 60$ torr

action is 1400°C or higher without a metal catalyst.^[12] These observations partially supported our point that CH_4 may not be fully cracked in our CVD chamber at 1000°C or lower, which affects the phase equilibria in the chamber and thus the phases of the bonding layer.

It should be noted that there is no stable phase region for the Ti_2O_3 compound in Fig. 5 to explain the formation of

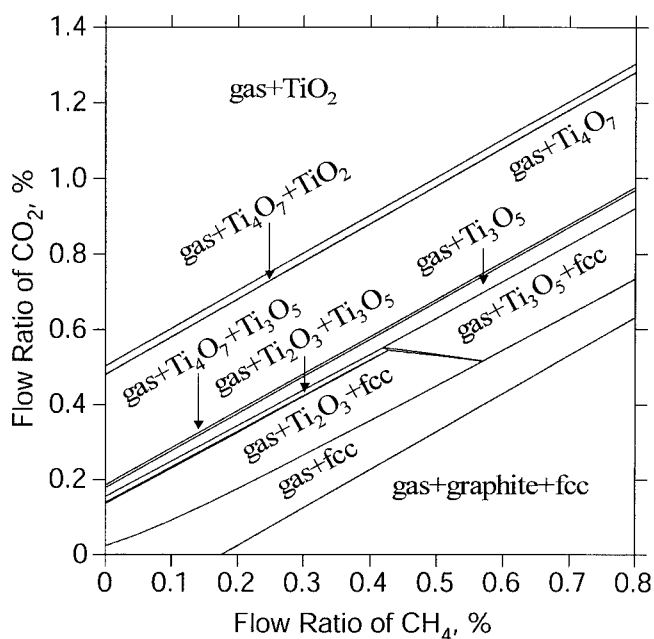


Fig. 7 Effect of CO_2 and CH_4 on the formation of titanium oxides with TiCl_4 flow ratio = 0.1%, $T = 970^\circ\text{C}$, and $p = 60$ torr

the Ti_2O_3 compound in one of the samples at the top of the CVD chamber. In this sample, a mixture of Ti_3O_5 and Ti_2O_3 were found. This suggests that the formation of the mixtures of titanium oxides is not only influenced by the flow ratio of CH_4 , but also other factors. CO_2 and TiCl_4 are two important precursors to provide O and Ti atoms that form titanium oxides. Figures 6 and 7 show the diagrams of CO_2 versus CH_4 flow ratios while the flow ratio of TiCl_4 changes from 0.3 to 0.1%, respectively. The following stable phase regions can be observed with decreasing CO_2 flow ratio: gas+ TiO_2 , gas+ Ti_4O_7 + TiO_2 , gas+ Ti_4O_7 , gas+ Ti_4O_7 + Ti_3O_5 , gas+ Ti_3O_5 , and gas+ Ti_2O_3 + Ti_3O_5 . As the formation of titanium oxides consumes CO_2 and TiCl_4 , the actual growth condition moves from the gas+ TiO_2 phase region at the bottom of the CVD chamber to the gas+ Ti_2O_3 + Ti_3O_5 region at the top of the CVD chamber. This explains the observation of the mixture of Ti_2O_3 + Ti_3O_5 , thus providing further evidence to support the hypothesis that a portion of CH_4 does not crack or participate in chemical reactions in the CVD chamber.

4. Conclusions

Thermodynamic calculations were conducted to explore the phase stability in the bonding layer of CVD coated

cemented carbide cutting tools. In comparison with experimental observations, it was found that less than 45% of CH_4 is active in chemical reactions and the rest may have not cracked at the experimental temperature range. The change of oxide mixtures from the bottom to the top of the CVD chamber can be explained by the consumption of Ti and O in the gas due to the formation of titanium oxides during the gas flow from the bottom to the top.

Acknowledgments

The authors gratefully acknowledge support from Kenametal, Inc., and partial financial support from the National Science Foundation through a CAREER Award (DMR-9983532).

References

1. S. Rупpi, Advances in Chemically Vapour Deposited Wear Resistant Coatings, *J. Phys. IV*, 2001, 11, p 847-859
2. A. Larsson, M. Halvarsson, and S. Vuorinen, Microstructure Investigation of As-Deposited and Heat-Treated CVD Al_2O_3 , *Surf. Coat. Technol.*, 1997, 94-95, p 76-81
3. M. Halvarsson, H. Norden, and S. Vuorinen, The Microstructure of Bonding Layers for CVD Alumina Coatings, *Surf. Coat. Technol.*, 1994, 68, p 266-273
4. Z.J. Liu, Z.K. Liu, C. McNerny, P. Mehrotra, and A. Inspektor, Investigations of the Bonding Layer in Commercial CVD Coated Cemented Carbide Inserts, *Surf. Coat. Technol.*, 2005 198, p 161-164
5. M. Halvarsson and S. Vuorinen, The Influence of the Nucleation Surface on the Growth of CVD Alpha- Al_2O_3 and Kappa- Al_2O_3 , *Surf. Coat. Technol.*, 1995, 76, p 287-296
6. T. Ishii, N. Shima, H. Ueda, S. Okayama, and M. Gonda, Microstructural Investigation of Alpha- Al_2O_3 -Epitaxially Coated Cemented Carbide Cutting Tools *J. Vac. Sci. Technol. A-Vac. Surf. Films*, 2001, 19, p 633-639
7. J.O. Andersson, T. Helander, L.H. Hoglund, P.F. Shi, and B. Sundman, THERMO-CALC & DICTRA, Computational Tools for Materials Science, *CALPHAD*, 2002, 26, p 273-312
8. Scientific Group Thermodata Europe (SGTE), Thermodynamic Properties of Inorganic Materials, in *Landolt-Börnstein New Series, Group IV, Lehrstuhl für Theoretische Hüttenkunde*, Springer-Verlag, Berlin, Heidelberg, 19, 1999
9. FEDATA, TCS/TT Steels Database, Version 1, ThermoCalc, Stockholm, Sweden, 1996, http://www.thermocalc.com/Products/databas_ny/FEDATA.htm
10. B.J. Lee and N. Saunders, Thermodynamic Evaluation of the Ti-Al-O Ternary System, *Z. Metallkd.*, 1997, 88, p 152-161
11. L. Fulcheri and Y. Schwob, From Methane to Hydrogen, Carbon-Black and Water, *Int. J. Hydrogen Energy*, 1995, 20, p 197-202
12. N. Muradov, Hydrogen via Methane Decomposition: an Application for Decarbonization of Fossil Fuels, *Int. J. Hydrogen Energy*, 2001, 26, p 1165-1175